J Solid State Electrochem (2011) 15:99–103
DOI 10.1007/s10008-010-1062-4

ORIGINAL PAPER

A tungsten oxide-based photoelectrocatalyst for degradation of environmental contaminants

Donald E. Macphee · Daniel Rosenberg · Matt G. Skellern · Richard P. Wells · John A. Duffy · Kenneth S. Killham

Received: 12 March 2010 / Revised: 24 March 2010 / Accepted: 25 March 2010 / Published online: 20 April 2010

Abstract The use of photocatalysts in the remediation of contaminated water is now well established in the scientific literature, the most common photocatalyst being nano-dimensional particulate titanium dioxide. The generation of charge and charge transfer mechanisms on titanium dioxide are also well described, but this paper addresses the use of tungsten oxide and discusses its potential in water remediation when supported as a photoelectrocatalytic electrode. A photoelectrocatalytic cell is described and its performance in the context of the band structure of tungsten oxide is discussed.

Introduction

In the last 5 years, the global water supply industry has spent >£57 billion on purification treatments. With an increasing population and a growing demand for clean water, this level of investment will increase over the next 10 years as the industry moves towards more efficient and sustainable processes for the treatment of a range of robust contaminants derived from agricultural processes (herbicides/pesticides), sewage (oestrogens, pathogens, etc.), industrial effluents (e.g. chlorinated phenolics) and natural runoff (soil- and plant-derived colourants).

Existing treatments based on activated carbons, ozone and UV processes are cost-intensive and have unfavourable environmental impacts. Photocatalytic processes have long been recognised as being aggressive towards organic pollutants and have wide applicability, but reactor designs are often complex and degradation rates and efficiencies tend to be low. This paper describes the coupling of photocatalysis with electrochemistry to supplement and enhance the effectiveness of photocatalysts. This is not in itself a novel integration of these processes, but the tungsten oxide-based materials being employed are found to have improved performance in such a configuration and are active in visible rather than UV light, which is normally necessary for photocatalysis. In common with other electrochemical cells, including those configured as fuel cells, the coupled process generates an electrical current during the pollutant degradation process.

It is through this aspect cell development that we are indebted to Dr. Fritz Baucke for his enthusiastic support in discussions relating to the redox behaviour of tungsten oxides [1] and their applications. Indeed, the electrochemical cell described in this paper has much in common with the electrochromic mirror [2–4] developed by Dr. Baucke and colleagues.

Photocatalytic processes and the photoelectrocatalytic fuel cell

Conventional nano-dimensional semiconductor photocatalysts degrade organic pollutants through a series of charge transfer processes. Illuminating radiation of energy greater than or equal to E_g, where E_g is the band gap for the material, generates electrical charge carriers in the material (Fig. 1) by promoting electrons to the (empty) conduction band, thereby leaving a corresponding number of holes in the valence band. These photogenerated charge carriers, provided they do not recombine with each other, promote a sequence of surface reactions as shown in Fig. 1, which

D. E. Macphee (✉) · D. Rosenberg · M. G. Skellern · R. P. Wells · J. A. Duffy · K. S. Killham
Departments of Chemistry and Plant & Soil Science,
University of Aberdeen,
Aberdeen, UK
e-mail: d.e.macphee@abdn.ac.uk

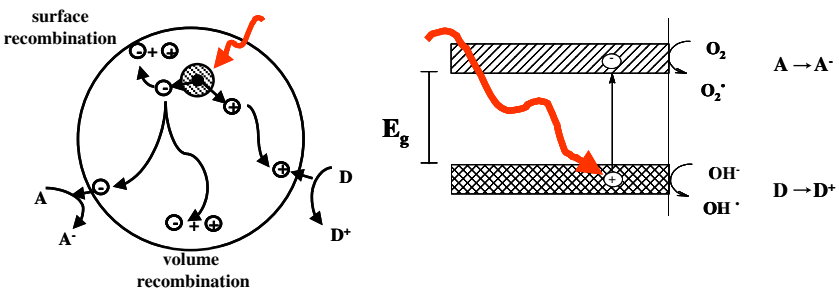

Fig. 1 Photocatalytic processes

ultimately lead to the mineralisation of the contaminant. Amongst the key processes on the catalyst surface are:

(a) reaction between the photogenerated hole (h^+) and water to produce the aggressively oxidising hydroxy radical ($OH^\bullet$),

$$H_2O_{(ads)} + h^+ \rightarrow H^+ + OH^\bullet{}_{(ads)}$$

(b) reaction between the photogenerated electron and adsorbed oxygen to produce the oxygen radical ($O_2^\bullet$),

$$e^- + O_{2(ads)} \rightarrow O_2{}^\bullet.$$

Further reactions from scheme (i) can lead to $HO_2^\bullet$, HO_2^- and H_2O_2, all of which can promote oxidising reactions with oxidisable species.

In addition, the oxidisable species themselves may be adsorbed onto the catalyst surface leading to reactions analogous with scheme (i), e.g. for methanol, $CH_3OH_{(ads)} + h^+ \rightarrow CH_3O^\bullet{}_{(ads)} + H +$.

The radicals arising from scheme (i)-type processes are highly reactive and can oxidise a wide variety of organic substances in multiple-step surface reactions.

The photoelectrocatalytic fuel cell (PECFC), shown schematically in Fig. 2, supports the catalyst on an electronically conducting substrate to provide a semiconducting anode. This anode is separated from a cathode by an electronically insulating membrane through which protons generated during scheme (i)-type processes and other pollutant degradation reactions are conducted (PCM). Some of the scheme (ii) processes ($A \rightarrow A^-$) are blocked in this cell because the photogenerated electrons can also be drawn from the catalyst, via the substrate and an external circuit, by the positive potential provided by a cathode reaction. This leaves the particularly aggressive oxidising species, the hydroxy radical ($OH^\bullet$), to form as the predominant photocatalytic oxidiser in the photoelectrocatalytic fuel cell (see Fig. 2). The cathode provides the reactive surface for protons arriving from the PCM to recombine with electrons from the external circuit in the presence of a reducable species, e.g. for oxygen $4H^+ + O_2 + 4e^- \rightarrow 2H_2O$.

Redox processes in the photoelectrocatalytic fuel cell

Consideration of the chemistry of tungsten oxide reveals a second potential mechanism for pollutant degradation. W^{6+}

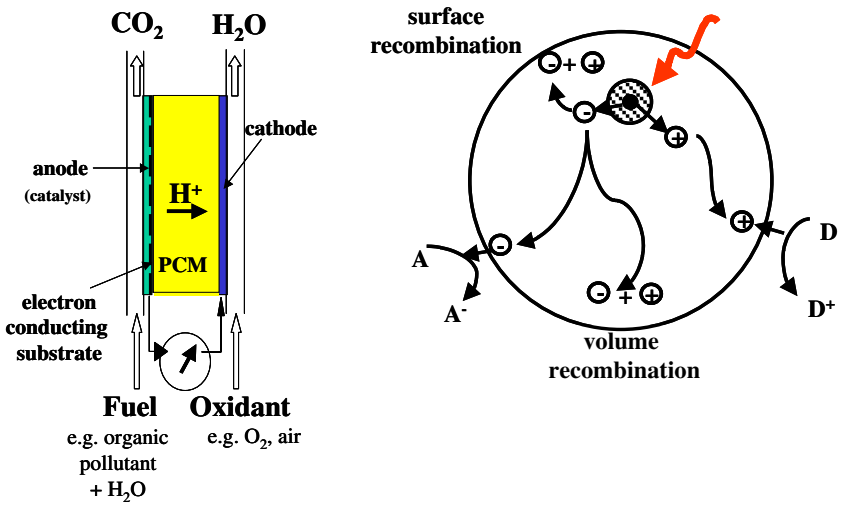

Fig. 2 Photocatalytic processes in the PECFC

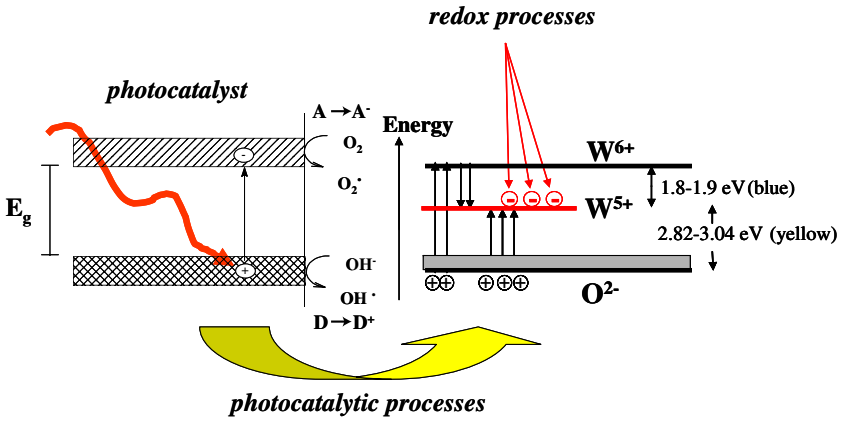

Fig. 3 Photoelectrocatalytic processes in the PECFC

is a strong oxidising agent and is readily reduced to W^{5+}, so a useful starting position is to consider the band structure of WO_3 in a partially reduced state. Figure 3 shows the band structure diagram which features a donor level, arising from the $5d^1$ configuration of W^{5+}, between the valence (O^{2-}) and the conduction (W^{6+}) bands. In effect, WO_3, a semiconductor, is also an oxidising agent, as is demonstrated by its readiness to convert to a 'bronze', the overall process being represented by scheme (iii):

$$e^- + H^+ + WO_3(\text{yellow}) \Leftrightarrow H_xW^{6+}{}_{(1-x)}W^{5+}{}_xO_3(\text{blue}).$$

Here, tungsten is present in mixed oxidation states. The associated colour change from yellow to blue is explained in terms of the band structure diagram (Fig. 3). The reduction of W^{6+} to W^{5+} populates the donor level and accounts for the yellow colour due to absorption of light with energies in the range 2.8–3.0 eV [5]. Transitions from the donor level to the conduction band (1.8–1.9 eV) correspond to the observed blue colour.

Whilst it is reasonable to view 'bronze' formation (scheme (iii)) as a mechanism for reduction of WO_3 in tandem with photocatalytic processes (which provide H^+, via scheme (i)-type reactions, and electrons) it is also appropriate to consider alternatives. W^{6+} is expected to have a considerable polarising potential and will strongly polarise electron density on neighbouring ions or molecules. It is therefore not unreasonable to propose that an electron donor (D) adsorbed on the surface of WO_3 for example, or on a hydrolysed WO_3 surface consisting of

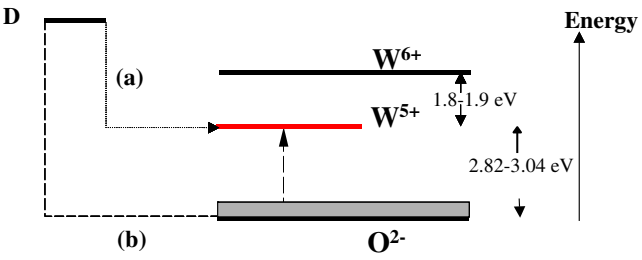

Fig. 4 Redox processes involving WO_3

W–O–H linkages, would be oxidised to develop the mixed oxidation state compound, $D^+{}_xW^{6+}{}_{(1-x)}W^{5+}{}_xO_3$ either by direct interaction with tungsten (route (a), Fig. 4) or via adjacent oxide ions (route (b), Fig. 4). This process is analogous to the description given above for the reaction between methanol and a photogenerated hole on a photocatalyst surface, but in this scenario, methanol donates its electron into the donor level of the tungsten oxide band structure (see 'redox processes' in Fig. 3). It can be envisaged that provided a sufficient driving force for such a process remains, the partially oxidised, chemisorbed methanol will continue to donate electrons as it is degraded finally to CO_2 and water. So, in principle, redox mechanisms can be offered to explain the oxidising potential of WO_3 even in the absence of photocatalytic processes.

Electrons promoted by light absorption may also be important in supporting redox processes. The sustainability of electron transfer processes may be somewhat sluggish if the population density of the donor level is low, as may be expected if there is insufficient overlap of occupied 5*d* (W) orbitals. However, under illumination, electrons promoted from the valence band increasingly occupy these orbitals to the point where, in principle, the semiconductor electrode could become metallic (a Mott transition). At this point, electron flow in the catalyst is increased and photocatalytic and redox processes are expected to become more efficient such that performance under illumination can be expected to be improved with light intensity. However, as the population density of the donor increases, the oxidising power of $H_xW^{6+}{}_{(1-x)}W^{5+}{}_xO_3$ decreases, so tendency for electron injection directly into the donor level is reduced as x increases, and the transition to metallic behaviour by this mechanism is unlikely in practice.

Cell dynamics

Continuous population of the W^{5+} level by both redox and photocatalytic processes will drive the W^{5+}/W^{6+} ratio upwards

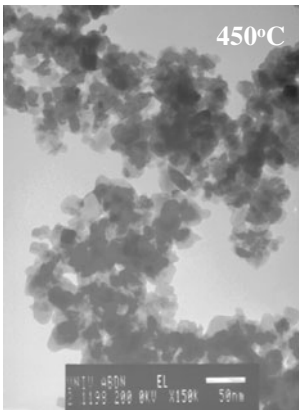

Fig. 5 TEM image of tungsten oxide-based catalyst

and reduce the oxidising power of the catalyst. This cannot be sustained because some saturation level will be achieved, which will be defined by the prevailing redox conditions. One advantage of the PECFC configuration is that cathode processes provide a mechanism for draining the W^{5+} level through the external circuit. Withdrawal of these electrons re-oxidises W^{5+} to W^{6+}, providing catalyst regeneration.

The driving force for electron withdrawal from the catalyst is provided by the potential difference between the catalyst electrode (anode) and the more positive cathode. The half-cell potential at the cathode is derived from the reduction of oxygen on Pt (ideally 1.23 V vs SHE). The anode potential is provided by an average of the equilibrium W^{5+}/W^{6+} activity ratio and ratios of other oxidised to reduced species.

Although anode half-cell potentials cannot strictly be estimated from the Nernst equation (because we are not dealing with activities of ions in solution), Nernstian treatments can be applied to monitor trends in potential. This is because the semiconductor's Fermi level correlates with its Nernst-derived potential, and consequently, as the W^{5+}/W^{6+} activity ratio increases, a negative shift in potential is expected (as predicted by the Nernst equation for the analogous aqueous system.

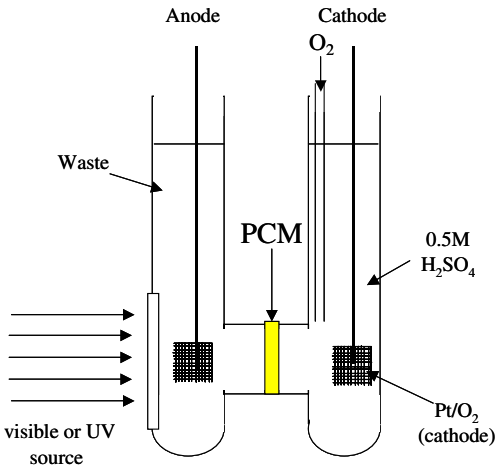

Fig. 6 PECFC configuration

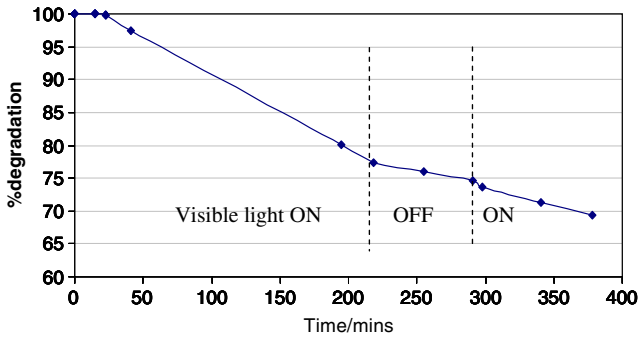

Fig. 7 PECFC response to a methylene blue solution (initially 5 ppm). Catalyst area was approximately 6 cm^2; initial cell current was approximately 14 μA

Experimental verification

As indicated above, the PECFC is therefore capable, in principle, of supporting at least two mechanisms for degradation of organic pollutants (electron donors). Preliminary studies using a range of organic materials, including chlorinated phenolics and naphthalene (a model for PAHs) and its oxidation products, have been encouraging, and these results are discussed below.

Preparation of materials and construction of the test cell

The PECFC is composed of a photocatalyst-assisted anode, cathode and proton conducting membrane (PCM). The central component is the PCM, fabricated using the sol–gel process described by D'Apuzzo et al. [6]. Tetraethylorthosilicate in ethanol (TEOS, EtOH, H2O, HCl (1:4:2:0.01)) was mixed with phosphoryl chloride (POCl3,EtOH (1:6)) with continuous stirring to give a sol of final composition $70SiO_2{:}30P_2O_5$ which was poured into moulds prior to gelling at around 24 h. Early preparations suffered from dimensional instability on drying over several weeks, leading to cracking, so subsequent membranes were made by grinding previously formed, cracked glass and pressing the powder into cylindrical forms (25-mm diameter, 100 MPa). The mechanically compacted discs were then partially sintered by firing at 750 °C for 2 h. Sintered discs were then repeatedly impregnated with fresh sol until when dried at 100 °C, air permeability from a manometer (water head of 400 cm) was negligible. Normally, ten impregna-

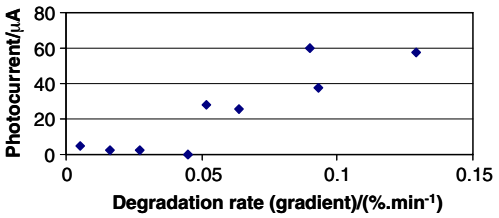

Fig. 8 PECFC current vs methylene blue degradation rate

tions were required to seal the interconnected porosity, and subsequent ac impedance measurements indicated a disc conductivity of 1.8×10^{-2} S cm^{-1} (compared with 8×10^{-2} S cm^{-1} for Nafion®, the state-of-the-art proton conductor).

A commercial cation exchange resin (Dowex 50 WX 4-50) was immersed in an acid solution (HCl 1 M), washed with double distilled water several times and packed uniformly in a glass column. After further washing (to pH 7), sodium tungstate solution (100 cm^3, 0.15 M) was run through the column (10 ml/min) and collected in ethanol (50 ml) under constant magnetic stirring. The eluted solution was partially evaporated under reduced pressure until it reached one tenth of its original volume upon which polyethylene glycol (PEG-300) was added as a particle growth inhibitor (WO_3/PEG ratio was varied between 0.2 and 0.8, *w*/*w*).

The solution obtained was left under constant mixing for 1 day to allow particles to reach the maximum critical size. After 24 h, the resulting mixture was spread on Petri dishes and placed in a furnace (100 °C, 10 min). The relatively viscous gel resulting was treated at 450 °C for 30 min to provide nanoparticulate green-yellow powders of relatively constant particle size (approx. 20 nm; Fig. 5). Due to the flammability of the gel, only small amounts were calcined and only in static air furnaces. Electron microscopy revealed particle size dependence on temperature (Fig. 5)

Anode and cathode electrodes consisted of platinum mesh, although in some cases, a gold-coated slide was used for the anode. Catalyst was electrophoretically deposited onto the anode directly from the PEG suspension and the anode assembly supported in the anode compartment of the cell (Fig. 6). A platinised platinum cathode was supported in a 0.5 M H_2SO_4 solution in the cathode compartment. The anode was supported in the anode compartment containing an aqueous solution of target 'pollutant'.

PECFC proof of principle

Figure 7 shows the performance of the PECFC using methylene blue as an oxidisable solute. It is acknowledged that other factors can lead to loss of methylene blue concentration in solution, e.g. photolysis and adsorption, but the obvious gradient change indicated between light and dark conditions, coupled with the recovery of a cell current, are consistent with the mechanisms suggested above for photoelectrocatalytic degradation of methylene blue, particularly as the rate of degradation (gradient) is proportional to the measured cell current (Fig. 8).

In addition to demonstrating efficient degradation of methylene blue, the PECFC has also shown effectiveness against colourants (blanket peatwater), chlorinated phenolics (2,4-dichlorophenol and pentachlorophenol), naphthalene and *Escherichia coli* 0157. The configuration of the PECFC has undergone several modifications since the time of Prof. Baucke's involvement. The phosphosilicate-based PCM has been replaced with Nafion® and membrane electrode assemblies integrating the WO_3-based anode are now produced for contemporary PECFC studies. More rigorous characterisation of the PECFC is reported in recent publications [7, 8].

Conclusions

The chemistry of tungsten oxide has been exploited in a photoelectrocatalytic cell (configured as a 'fuel cell') capable of oxidative degradation of organic pollutants in its anode compartment. The electrochemistry has similarities to that employed in the electrochromic mirror of Prof. Baucke and colleagues [2–4], but the quite different application provides an opportunity for the sustainable (solar-assisted) remediation of organic-contaminated water bodies due to the specific bonding characteristics (band structure) of the active tungsten bronze anodic catalyst. Under visible light illumination, the cell has demonstrated degradation of a range of recalcitrant environmental contaminants whilst generating a cell current. The rate of degradation is dependent on illumination level and is proportional to the cell current produced as demonstrated in this paper for methylene blue solutions. This behaviour is consistent with the mechanisms discussed based on cell dynamics and underlying tungsten oxide chemistry.

Acknowledgments The authors gratefully acknowledge financial support from the University of Aberdeen, Scotoil Services Ltd and Scottish Enterprise Grampian.

References

1. Baucke FGK, Duffy JA, Smith RI (1990) Optical absorption of tungsten bronze thin films for electrochromic applications. Thin Solid Films 186:47–51
2. Baucke FGK, Bange K, Gamgke T (1988) Reflecting electrochromic devices. Devices 9:179–187
3. Baucke FGK (1987) Electrochromic mirrors with variable reflectance. Solar Energy Mat 16:67–77
4. Baucke FGK, Duffy JA (1986) Darkening glass by electricity. Chem Br 21:643–646
5. Goodenough JB (1971) Metallic oxides. Prog Solid State Chem 5:145–399
6. D'Apuzzo M, Aronne A, Esposito S, Pernice P (2000) J Sol–Gel Sci Technol 17:247
7. Nissen S, Alexander BD, Dawood I, Tillotson M, Wells RPK, Macphee DE, Killham K (2009) Remediation of a chlorinated aromatic hydrocarbon in water by photoelectrocatalysis. Environ Pollut 157:72–76
8. Macphee D, Wells R, Kruth A, Todd M, Elmorsi T, Smith C, Pokrajac D, Strachan N, Mwinyhijad M, Scott-Emuakpord E, Nissen S, Killham K (2009) A visible light driven photoelectrocatalytic fuel cell for clean-up of contaminated water supplies. Desalination 248:132–137